THE JOURNAL OF BIOLOGICAL CHEMISTRY
Vol. 279, No. 17, Issue of April 23, pp. 17459–17465, 2004
Printed in U.S.A.

Conformational Changes in the Reaction of Pyridoxal Kinase*

Received for publication, November 12, 2003, and in revised form, February 2, 2004
Published, JBC Papers in Press, February 5, 2004, DOI 10.1074/jbc.M312380200

Ming-hui Li‡, Francis Kwok§, Wen-rui Chang‡, Sheng-quan Liu‡, Samuel C. L. Lo§, Ji-ping Zhang‡, Tao Jiang‡¶, and Dong-cai Liang‡

From the ‡National Laboratory of Biomacromolecules, Institute of Biophysics, Chinese Academy of Sciences, Beijing 100101, China, §Department of Applied Biology Chemical Technology, Hong Kong, China and Polytechnic University, Hung Hom, Kowloon, Hong Kong, China

To understand the processes involved in the catalytic mechanism of pyridoxal kinase (PLK),[1] we determined the crystal structures of PLK·AMP-PCP-pyridoxamine, PLK·ADP·PLP, and PLK·ADP complexes. Comparisons of these structures have revealed that PLK exhibits different conformations during its catalytic process. After the binding of AMP-PCP (an analogue that replaced ATP) and pyridoxamine to PLK, this enzyme retains a conformation similar to that of the PLK·ATP complex. The distance between the reacting groups of the two substrates is 5.8 Å apart, indicating that the position of ATP is not favorable to spontaneous transfer of its phosphate group. However, the structure of PLK·ADP·PLP complex exhibited significant changes in both the conformation of the enzyme and the location of the ligands at the active site. Therefore, it appears that after binding of both substrates, the enzyme-substrate complex requires changes in the protein structure to enable the transfer of the phosphate group from ATP to vitamin B_6. Furthermore, a conformation of the enzyme-substrate complex before the transition state of the enzymatic reaction was also hypothesized.

Pyridoxal kinase (PLK)[1] catalyzes the phosphorylation of vitamin B6 (including pyridoxal, pyridoxine, and pyridoxamine) in the presence of ATP and Zn^{2+}, which is an essential step in the synthesis of pyridoxal 5′-phosphate (PLP), an active form of the vitamin in mammals (1–3). PLK is expressed in all mammalian tissues because of the fact that PLP cannot cross cell membranes, and PLK is required for the activation process inside cells (4). Genes encoding PLK have been cloned from both mammalian and plant cells. PLK activity has also been detected in bacteria, because PLP can be synthesized through the PLP salvage pathway (5, 6).

Recently, the three-dimensional structures of PLK from sheep brain and its complex with ATP were determined (7). Although structural analyses have shown that PLK exhibits a folding pattern similar to the core structure of enzymes in the ribokinase superfamily (8–13), low sequence homology between the two types of enzymes has been found. Despite kinetic studies that have shown that ribokinase and adenosine kinase both follow an ordered substrate-binding mechanism, PLK binds ATP and pyridoxal randomly (8, 10, 14). During the binding of ATP, a flexible loop containing 12 amino acid residues in the active site of PLK was responsible for triggering a major conformational change of the protein structure by interacting with the bound ATP. It has been suggested that the purpose for the inability of ATP to interact with this loop before catalysis is to prevent the nucleotide from hydrolysis, which is an essential feature in the random substrate binding mechanism.

Further interest in crystallographic studies of PLK in the presence of substrates has arisen from several considerations. First, the structure of PLK complexes in the presence of pyridoxal has never been revealed. Thus, the exact interactions between molecules in the active site of PLK are unknown. Secondly, in the PLK·ATP complex, ATP γ-phosphate group is maintained in a position far away from the catalytic site of the enzyme. Although this could prevent the nucleotide from hydrolyzing, the enzyme would need to engineer a dramatic conformational change of this macromolecule for the transfer process. This contradicts the design of other kinases found in nature, indicating that cells may have some regulatory mechanism to control PLK activity. Finally, the catalytic process of PLK consists of several steps. The structure of PLK in the form of a complex with different substrates or its analog and products allows the systematic observation of reaction cycles. In this paper, the crystal structures of the PLK·AMP-PCP-pyridoxamine complex, the PLK·ADP·PLP complex, and the PLK·ADP complex were determined. These structures have provided detailed information regarding the interactions between PLK and its substrates or products. Comparison of these structures can lead to a thorough understanding of conformational changes that occur in the enzyme in the presence the ligands in this unique phosphorylation process catalyzed by PLK.

MATERIALS AND METHODS

Crystallization and Data Collection—PLK was purified from sheep brain as described previously (1). Enzyme crystals were obtained by using the hanging drop vapor diffusion method at a constant temperature of 17 °C.

An initial attempt to diffuse AMP-PCP and pyridoxamine into the native orthorhombic crystals of the enzyme was not successful. However, co-crystallization of PLK in the presence of AMP-PCP and pyridoxamine resulted in the formation of crystals of the enzyme-substrate complex. A solution was prepared consisting of 10 mg/ml PLK, 1 mM

* This work was supported by the National Natural Science Foundation of China (Grant 30100026), the Life Science Special Fund of Chinese Academy of Services (Grant STZ0017), and the National Key Research Development Project of China (Grant G1999075601). The costs of publication of this article were defrayed in part by the payment of page charges. This article must therefore be hereby marked "*advertisement*" in accordance with 18 U.S.C. Section 1734 solely to indicate this fact.

The atomic coordinates and structure factors (code 1RFT for PLK·AMP-PCP-pyridoxamine, 1RFU for PLK·ADP·PLP, and 1RFV for PLK·ADP) have been deposited in the Protein Data Bank, Research Collaboratory for Structural Bioinformatics, Rutgers University, New Brunswick, NJ (http://www.rcsb.org/).

¶ To whom correspondence should be addressed: National Laboratory of Biomacromolecules, Institute of Biophysics, Chinese Academy of Sciences, 15 Datun Rd., Chaoyang District, Beijing 100101, China. Tel.: 86-10-64888510; Fax: 86-10-64889867; E-mail: x-ray@sun5.ibp.ac.cn.

[1] The abbreviations used are: PLK, pyridoxal kinase; PLP, pyridoxal 5′-phosphate; AMP-PCP, adenosine 5′-(β,γ-methylenetriphosphate); r.m.s.d., root mean square deviation.

TABLE I
Structure determination and refinement

	PLK·AMP-PCP-pyridoxamine	PLK·ADP·PLP	PLK·ADP
Data collection statistics			
Space group	$P3_121$	$P4_3$	$P2_12_12_1$
Cell dimension	$a = b = 103.7$, $c = 58.6$	$a = b = 109.1$, $c = 284.3$	$a = 59.1$, $b = 93.9$, $c = 128.7$
Resolution (Å)	2.8	2.8	2.8
Measured reflections	48,149	342,212	101,511
Unique reflections	9,133	75,513	18,118
Completeness (%)	99.6 (100)	87.5 (95.2)	99.6 (99.9)
R_{merge} [a]	0.110 (0.543)	0.0867 (0.465)	0.136 (0.559)
$\langle I / \sigma(I) \rangle$	15.7 (3.4)	11.4 (2.3)	13.0 (3.0)
Refinement statistics			
R_{work} [b]	0.214	0.229	0.190
R_{free} [c]	0.268	0.281	0.222
Number of protein atoms	2,413	19,512	4,798
Number of ligand atoms	45	344	56
R.m.s.d. bonds (Å)	0.010	0.010	0.007
R.m.s.d. angles (°)	1.5	1.5	1.3
Average B-factor (Å^2)			
Protein atoms	30.2	36.0	30.0
Ligand atoms	29.1	33.1	36.2
Solvent atoms	34.3	41.3	34.8

[a] $R_{merge} = \Sigma_h\Sigma_i(|I_i(h) - \langle I(h)\rangle|)/\Sigma_h\Sigma_i I_i(h)$, where $I_i(h)$ is the ith integrated intensity of a given reflection and $\langle I(h)\rangle$ is the weighted mean of all of the measurements of $I(h)$.
[b] $R_{work} = \Sigma_h||F(h)_o| - |F(h)_c||/\Sigma_h|F(h)_o|$ for the 90% of reflection data used in refinement.
[c] $R_{free} = \Sigma_h||F(h)_o| - |F(h)_o||/\Sigma_h|F(h)_o|$ for the 10% of reflection data excluded from refinement.

pyridoxamine, 1 mM AMP-PCP, and 0.1 mM zinc acetate with a buffer of equal volume consisting of 100 mM KH_2PO_4-K_2HPO_4 containing 1.4 M $(NH_4)_2SO_4$, pH 8.2. The solution was then equilibrated against the buffer containing 1.4 M ammonium sulfate, pH 8.2, for approximately one month at 290 K. Similar conditions were used for the crystallization of a PLK·AMP-PCP-pyridoxamine complex. When AMP-PCP was replaced by ADP and pyridoxamine was replaced by PLP, the PLK·ADP·PLP complex crystals were obtained. Interestingly, the PLK·AMP-PCP-pyridoxamine complex crystals were trigonal, whereas the PLK·ADP·PLP complex crystals were tetragonal. PLK·ADP complex crystals were prepared by soaking the orthorhombic crystal of native enzyme (15) in 75 mM KH_2PO_4-K_2HPO_4 buffer containing 1 mM ADP, 1 mM $ZnAc_2$, and 30% polyethylene glycol 6000, pH 6.5.

Data from PLK·AMP-PCP-pyridoxamine and PLK·ADP complex crystals were collected using the Mar345 image plate in the National Laboratory of Biomacromolecules (Beijing, China) at room temperature. Data from the PLK·ADP·PLP complex were collected on a Mar345 image plate in the Laboratory of Structural Biology, Tsinghua University (Beijing, China). Before data collection, the crystals were flash-frozen in liquid nitrogen after short soaking in a solution consisting of 17.5% glycerol, 1.4 M ammonium sulfate, and 100 mM potassium phosphate buffer at pH 8.2. All of the data were processed with the HKL suite of programs (16). Table I shows the data collection statistics.

Structural Analysis and Refinement—The structure of the PLK·AMP-PCP-pyridoxamine complex was solved by molecular replacement using AMORE (17). The solution was obtained using the unliganded structure (with residues 117–128 omitted) as a search model. Because diffraction intensities of this complex crystal were slightly dispersed and could affect the measurement of weak reflections, the refinement process was carried out using reflections only at above 2σ cutoff. After rigid body refinement, the R-factor was dropped to 0.293 and then pyridoxamine, AMP-PCP, zinc ions, and the missing water molecules were added. During model rebuilding, xyz and B-factor refinements were carried out alternately, resulting in an R-free of 0.268 in the presence of 22 additional water molecules.

The PLK·ADP·PLP complex crystal was initially indexed as $P4_32_12$, but was later found to be nearly perfectly twinned with a twinning ratio of 0.48 (18). Therefore, data were reprocessed in $P4_3$. The complex structure containing eight monomers in an asymmetric unit was solved by molecular replacement with the MOLREP (19) program. Refinement was performed using the CNS (20) scripts for twinning data, and non-crystallographic symmetry restraint was applied. Initial simulated annealing (21) changed the R-factor to 0.264, and an electron density map was calculated according to the structure to which PLP and ADP molecules had been added. After several cycles of xyz refinement, B-factor refinement, and model rebuilding, a model with an R-factor of 0.229 and an R-free of 0.281 were obtained.

The structure of the PLK·ADP complex was determined by the difference Fourier method using the unliganded structure (Protein Data Bank code 1LHP) as a model. Rigid body refinement reduced the R-factor from 0.339 to 0.245. The following cycles of xyz refinement, B-factor refinement, and model rebuilding including the addition of missing residues such as ADP molecules, Zn^{2+} ions, and water molecules resulted in an R-factor of 0.190 and R-free of 0.222.

All of the model rebuilding were performed by program O (22), and the models were evaluated using PROCHECK (23). Computing programs including MOLSCRIPT (20), RASTER3D (25), and GRASP (26) were utilized to draw figures.

RESULTS AND DISCUSSION

Structures of Pyridoxal Kinase in Complexes with Substrates and Products—In contrast with the orthorhombic crystals of native PLK and the PLK·ATP complex, the PLK·AMP-PCP-pyridoxamine crystal belongs to the $P3_121$ space group with the complex having one monomer in the asymmetric unit. However, the two monomers related by the 2-fold crystallographic axis form a dimeric molecule in a fashion similar to the dimeric molecules found in the native PLK structure. The overall structure of the monomeric PLK·AMP-PCP-pyridoxamine complex is almost identical to the structures of the enzyme in the absence of ligands and the PLK·ATP complex. Of the 309 residues, the Cα deviations of 287 residues are <1 Å with an r.m.s.d. of 0.43 Å. In the active site of the enzyme, AMP-PCP and pyridoxamine were located in substrate binding sites, as revealed by the electron density map (Fig. 1*a*). In the pyridoxal binding site, three hydrogen bonds formed between pyridoxamine and its surrounding amino acid residues. One bond formed between the hydroxyl group in the side chain of Ser-12 and N1 of pyridoxamine. The second bond formed between the hydroxyl group of Thr-47 and O3, and the third bond formed between the carboxyl group of Asp-235 and O5. Tyr-84 and Val-19 also interacted with the two sides of the pyridine ring of pyridoxamine through hydrophobic interactions (Fig. 2). In contrast to the structure of the PLK·ATP complex, which is missing the second substrate bound at the active site, our result showed that the side chain of Tyr-84 in the PLK·AMP-PCP-pyridoxamine complex was slightly closer to the nucleotide because of the fact that the position of Tyr was stabilized by a hydrogen bond between itself and the guanidino group of Arg-86. As for the amino acid residue of Phe-43, its phenyl ring rotated at an angle of ~80°. In addition, the Thr-47 hydroxyl group moved toward Phe-43, resulting in a shorter hydrogen

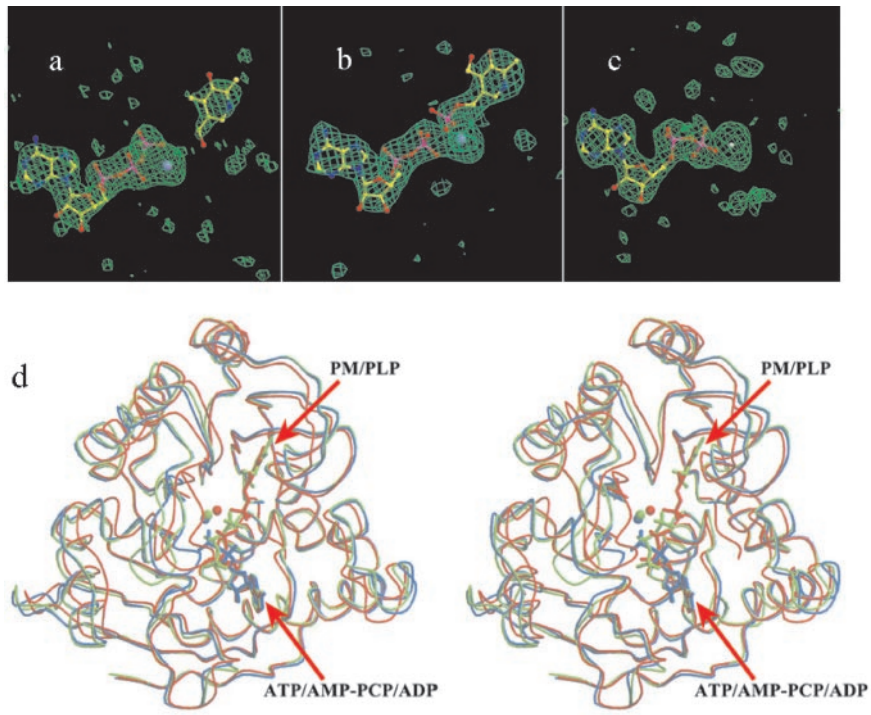

FIG. 1. **Structures of pyridoxal kinase in complexes with substrates or products.** *a*, *b*, and *c*, the $F_o - F_c$ electron density map contoured at 3σ using the reflection data for the PLK·AMP-PCP-pyridoxamine complex, for the PLK·ADP·PLP complex, and for the PLK·ADP complex, respectively, showing clear density for the ligands bound to the enzyme. *d*, the superposition of the main chain of the three complexes. The overall structure of the PLK·AMP-PCP-pyridoxamine complex (shown in *yellow*) is similar to that of the PLK·ADP complex (shown in *blue*) and is also similar to the PLK·ATP complex structure in which structure has already been solved. However, the PLK·ADP·PLP complex (shown in *red*) is significantly different from them, the peptide chain moves toward to the active center, and the overall structure becomes more compact.

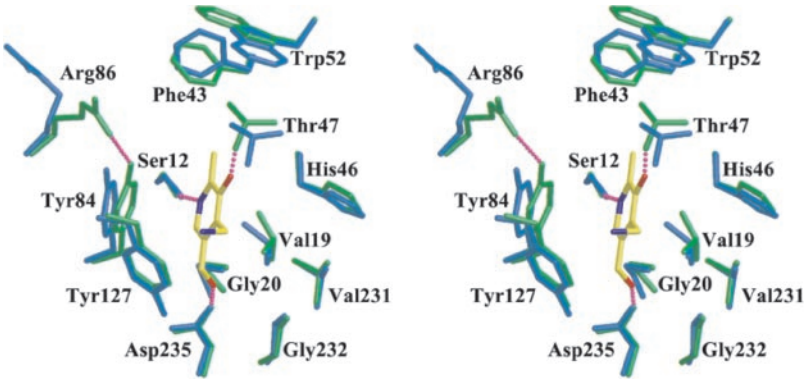

FIG. 2. **Pyridoxal binding site.** The molecule in the center is the pyridoxamine bound in the PLK·AMP-PCP-pyridoxamine complex. The surrounding residues are shown in *green*, and the hydrogen bonds between the pyridoxamine and the residues are shown as *purple dashes*. The corresponding residues in the PLK·ATP complex are in *blue*. A comparison of these structures reveals local conformational adjustments of the pyridoxal binding site when the substrates binds.

bonding distance between Thr-47 and O3 of pyridoxamine. A conformational change was detected in Trp-52, which is maintained in a position located adjacent to Phe-43 and Thr-47 with its indole ring made at a complete rotation of 180 degrees. Therefore, the relative side chain orientation between Phe-43 and Trp-52 changes from "edge-to-face" to "offset-stacked." At the nucleotide binding site, both the conformation of AMP-PCP and its interactions with surrounding amino acid residues were similar to those of ATP in the PLK·ATP complex.

Although the conditions for crystallization were similar to those of the PLK·AMP-PCP-pyridoxamine complex, the crystals of the PLK·ADP·PLP complex were tetragonal. Monomers of the two different enzyme-substrate complexes had significant conformation differences. Of a total of 309 amino acids, 117 residues in the PLK·ADP·PLP complex had α carbon atoms that deviated by >1 Å compared with the PLK·AMP-PCP-pyridoxamine complex. Such a dramatic variation in the conformation of the whole macromolecule could explain the generation of a new protein crystal form in the presence of different substrates. In the asymmetric unit of the PLK·ADP·PLP structure, eight monomers were found, forming four dimeric molecules in a manner similar to that of the native enzyme. An ADP molecule, a PLP molecule, as well as a Zn^{2+} ion bound at the active site of each monomer. The phosphate group of PLP and β-phosphate of ADP bridged by a Zn^{2+} ion were in close proximity to each other. The PLP phosphate group formed hydrogen bonds with the main chain nitrogen atoms of Gly-232, Thr-233, Gly-234, and Asp-235, as well as with the side chain of Asp-235 and Thr-127 (Fig. 3). Interactions between the other portions of the PLP molecule and the protein were similar to those in the PLK·AMP-PCP-pyridoxamine complex. PLP bound tightly in an area of the protein, which was structurally more compact than the same domain in the PLK·AMP-PCP-pyridoxamine complex (shown in Fig. 4*b* and discussed under "Results and Discussion"). Remarkably, neither the pyridoxamine 4′-amino group in the enzyme-substrate complex nor the PLP 4′-aldehyde group in the enzyme-product complex were found to be covered by any of the amino acid chains of the protein (Fig. 4*c*). This finding is in agreement with previous research that reported that substrate variation within this group did not affect the catalytic activity of PLK (3). In other words, the fact that the 4′-substitution group of the vitamin is exposed to the solvent explains the broad substrate specificity of PLK.

In the analysis of the structure of the PLK·ADP complex, an ADP molecule and a Zn^{2+} ion were found in the active site of each monomer. Since this complex could be used as a model to represent the reaction state in which the phosphate transfer process had been completed, the product, PLP, was released from the enzyme. The overall conformation of the protein in

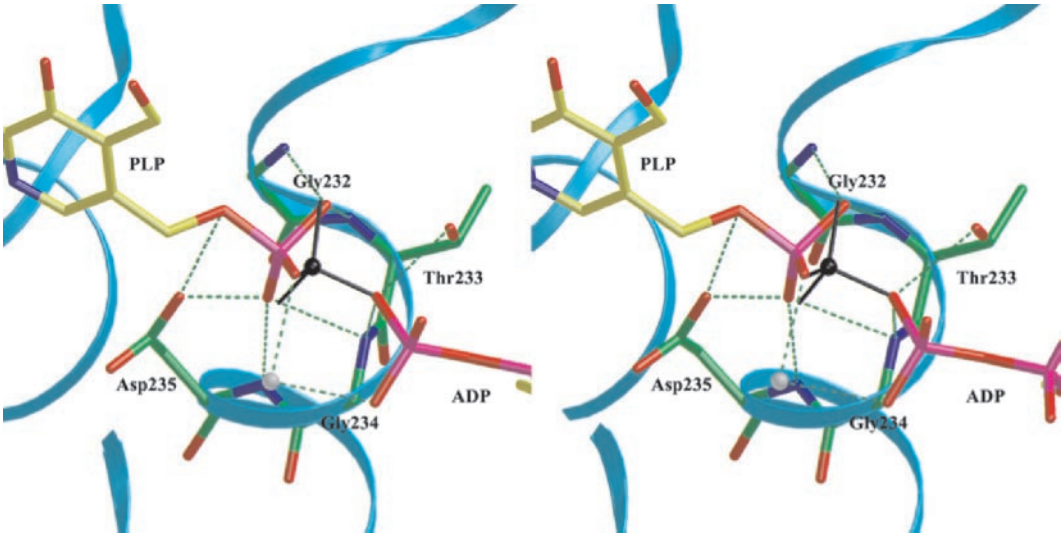

FIG. 3. **Pre-reaction state model based on the structure of the PLK·ADP·PLP complex.** In the PLK·ADP·PLP complex, the PLP phosphate group is located in the catalyzing site and makes hydrogen bonds with both the side chain carboxyl group of Asp-235 and the main chain nitrogen atoms of residue 232–235. These bonds created an anion hole. The distance between the PLP-phosphorus atom and the oxygen atom of the ADP β-phosphate is only 2.5 Å. The pre-reaction model can be constructed by moving the PLP-phosphorus atom toward ADP by 0.8 Å (shown in *black*) and connecting it to the ADP β-phosphate without a great adjustment of the other three oxygen atoms.

this complex was almost identical to that of the PLK·ATP complex (Fig. 1*d*) with an r.m.s.d. of only 0.25 Å for all of the residues with the exception of the loop 117–128. Compared with the compact structure of the PLK·ADP·PLP complex, the PLK·ADP complex has a relatively open conformation because the active site is exposed to the solvent region. In addition, the ADP molecule in this complex is significantly different from both ATP in the PLK·ATP complex and ADP in the PLK·ADP·PLP complex, primarily at the position of the phosphate groups. Compared with the ADP molecule in the PLK·ADP·PLP complex, α-phosphate of ADP in the PLK·ADP complex could move a distance of 1.1 Å, leading to its inability to form hydrogen bonds with Thr-186 and Asn-150. Instead, a new hydrogen bond was formed with Thr-233. Another movement of 2.2 Å was observed to have taken place on the β-phosphate, forming a new hydrogen bond with Thr-186 and decreasing its distance from Asp-118 (Fig. 5).

Reaction State before the Phosphate Transfer—In the PLK·ATP complex, the γ-phosphate of ATP is far away from the catalytic site. This prevents ATP from being hydrolyzed before pyridoxal is bound (7). Therefore, it was correct to expect that the binding of pyridoxamine would induce some form of conformational changes on both ATP and PLK, causing the γ-phosphate of ATP to be close to the other substrate. In the other location of the catalytic site of PLK, pyridoxamine should have also been bound in a position that allowed its 5′-hydroxyl group to be able to start a nucleophilic attack on ATP. However, in structural studies, neither AMP-PCP nor the enzyme in the PLK·AMP-PCP-pyridoxamine complex has exhibited any significant difference from the structure in the PLK·ATP complex and the γ-phosphorus atom was unusually far away from the 5′-hydroxyl oxygen atom. At a distance of 5.8 Å, it would be impossible for a spontaneous reaction of phosphate transfer to take place. Based on these findings, it could be hypothesized that there is another state of protein conformation known as the "pre-reaction state," which might take place just before the phosphate transfer so that the two substrates could be brought close enough together for the reaction to occur. Although this reaction state was not visible in the crystal structures of the enzyme-substrate complexes in this study, its existence could be proven based on the products formed in the reaction.

Based on what is known regarding protein chemistry, we believe that the conformation of the PLK·ADP·PLP complex is more similar to the conformation of the transition state (or the pre-reaction state) than to the conformation of the PLK·AMP-PCP-pyridoxamine complex. There are several reasons for this. First, the PLP phosphate group, which corresponds to the γ-phosphate of ATP before the reaction, is located in the catalytic site of PLK. It forms a hydrogen bond with the side chain carboxyl group of Asp-235 as well as with the main chain nitrogens of residues 232–235, which are skeletons of a positively charged anion hole. It is strongly believed that this hole plays a functional role in the stabilization of the transition state of the phosphate group (Fig. 3). Furthermore, β-phosphate of ADP is close to the PLP phosphate group that corresponds to the original positions of the β- and γ-phosphate of ATP before the reaction. The distance between ADP O1B atom and PLP-phosphorus atom was 2.5 Å (Fig. 4*a*). In the enzymatic reaction during phosphate transfer, the bond between O1B of ATP and the γ-phosphorus atom was broken and a new bond was subsequently formed between the phosphorus atom of the γ-phosphate group and the oxygen atom of the 5′-hydroxyl group of pyridoxal. These three atoms in the PLK·ADP·PLP complex were almost collinear (Fig. 3). The arrangement of molecules in this format is consistent with the S_N2 mechanism.

Therefore, a pre-reaction state model just before the formation of the transition state was constructed based on the structure of the PLK·ADP·PLP complex. The model was constructed by moving the phosphorus atom of PLP (in the structure of the PLK·ADP·PLP complex) by 0.8 Å along the line linking it to the O1B of ADP, and thus, a new bond between these two substrates was formed. At the same time, the bond between the phosphorus atom and oxygen atom within the PLP phosphate group was broken. The operation mentioned above would lead to the conversion of ADP and PLP to ATP and pyridoxal without requiring movement of other atoms in either ADP and PLP. Indeed, this process was the reverse of the phosphate transfer via the transition state in the reaction catalyzed by PLK.

Conformational Changes before the Reaction—Superposition of different ternary complexes of enzyme-substrate in this investigation revealed unusual changes in both the location and orientation of the two substrates. In contrast to the PLK·AMP-PCP-pyridoxamine complex, it is assumed that the molecule of

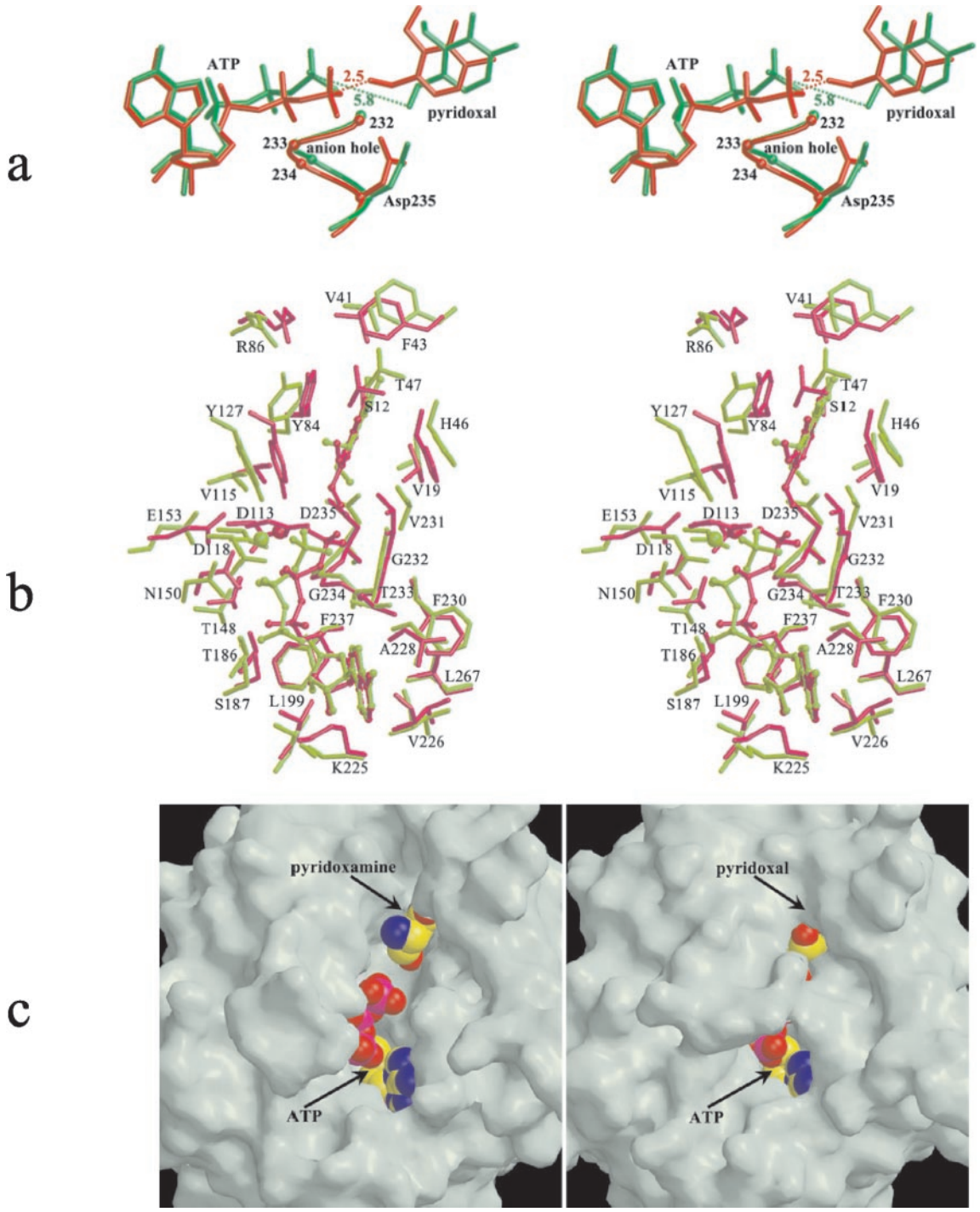

FIG. 4. **Structural changes before the reaction revealed by the comparison of the PLK·AMP-PCP-pyridoxamine structure and the pre-reaction model.** *a*, the substrates in the two structures. The two substrates in the PLK·AMP-PCP-pyridoxamine complex are far away from each other. The γ-phosphate of AMP-PCP is not in the anion hole, and its phosphorus atom is 5.8 Å away from the O5 atom of pyridoxamine. However, in the pre-reaction model, the γ-phosphate of ATP forms hydrogen bonds with the catalyzing residues and the distance between its phosphorus atom and the O5 atom of pyridoxamine is only 2.5 Å. *b*, structural changes of residues around the active site. In contrast with the PLK·AMP-PCP-pyridoxamine complex, the residues around the active site of the pre-reaction state model move toward the substrate and push them closer to each other. These residues bind the substrates tightly and restrict the reaction group in a suitable position for the phosphate transfer. *c*, surface presentation of the active site. The *left side* shows the PLK·AMP-PCP-pyridoxamine complex in which the active site is open. The *right side* shows pre-reaction state model in which the conformational changes cause the active site to move closer each other and the two substrates are almost buried totally. However, in both of these two structures, the 4′-substituted group of pyridoxamine or pyridoxal are exposed, which allows variations within this group.

pyridoxal in the pre-reaction state was translocated toward ATP at a distance of 1.4 Å. Similarly, some conformational adjustment should also occur on the pyridoxal 5′-hydroxyl group. Therefore, both the nitrogenous base and the ribose ring of ATP would have to maintain their positions in the active site, whereas conformational changes of the enzyme would take place to affect the stability of the ATP phosphate groups. As a result, translocations of 1.5 Å were detected for the β-phosphate group and translocations of 1.9 Å were detected for the γ-phosphate group. These movements would then enable the

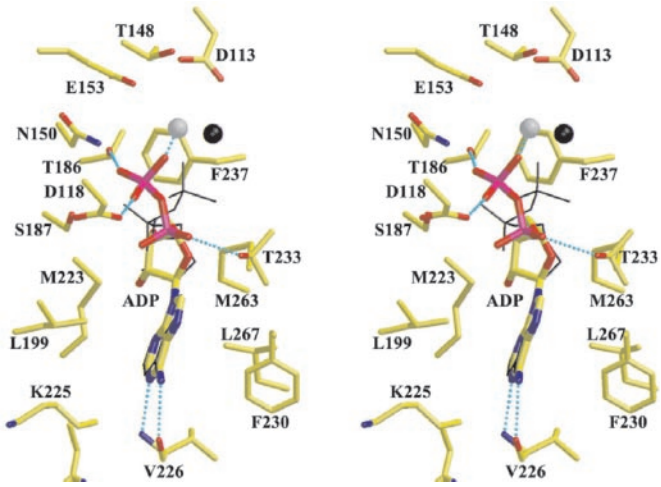

FIG. 5. **The ADP molecule bound in the PLK·ADP complex and the residues interacting with it.** The hydrogen bonds between them are shown as *blue dashes*. The molecule shown as a *thin black line* is the ADP in the PLK·ADP·PLP complex. A significant conformational change happens between the two ADP molecules.

two substrates to be placed in suitable positions for subsequent phosphate transfer.

Despite the movement of substrates, significant conformational changes were also observed in the protein structure (Fig. 4*b*). Unlike the structure of the PLK·AMP-PCP-pyridoxamine complex, over one-third of the Cα atoms in the PLK·ADP·PLP complex moved 1 Å or more. In addition, all of the atoms in helices α4, α5, and α6 were found to move ~1.5 Å. This type of movement enabled peptide chains within the protein to move toward the active site, thus creating a compact structure in the enzyme (Fig. 1*d*). In the pyridoxal binding site, the loop connecting β2 and α2 moved approximately 2 Å toward the substrate pyridoxal. This movement enabled residues Val-41, Phe-43, and Thr-47 on this loop to interact with pyridoxal directly and push pyridoxal toward the ATP. At the same time, Tyr-84, Tyr-127, His-46, Val-231, and Val-115 moved toward the pyridine ring of pyridoxal from two sides, causing immobilization of the substrate in the active site (Fig. 4*b*). Although small changes were detected at the ATP adenine ring, Leu-199, Lys-225, and Phe-230 also moved closer to ATP for the purpose of immobilization. Amino residues interacted with the ATP phosphate group either directly or via cations including Thr-186, Ser-187, Asn-150, Glu-153, Asp-113, Asp-118, Tyr-127, and Thr-148, which are mainly located on one side of ATP. The peptide chain consisting of these amino acid residues tends to move against the ATP molecule, pushing the γ-phosphate group to the anion hole previously formed by the main chain nitrogens of residues 232–235 at the N-terminal end of α7. Consequently, the phosphate was able to form new hydrogen bonds with these amino acid residues (Fig. 4*b*). Tyr-127 and Asp-118 in loop 117–128 interacted with the dorsal portion of ATP. Dramatic conformational changes of this loop would eventually shift these two residues to new positions where these residues would provide the ATP molecule with increased stabilization.

Mechanism of Pyridoxal Kinase—Two major catalyzing mechanisms have been suggested for enzymes belonging to the ribokinase superfamily. An anion hole with the ability to stabilize the transition state of reactants is formed by the main chain nitrogen atoms of several continuous residues (8, 10, 13). In PLK, such an anion hole is created by residues 232–235 at the N-terminal end of the α7 helix. A base-catalyzing group in the active site is needed to initiate the reaction through deprotonation of the hydroxyl group on the vitamin substrate so

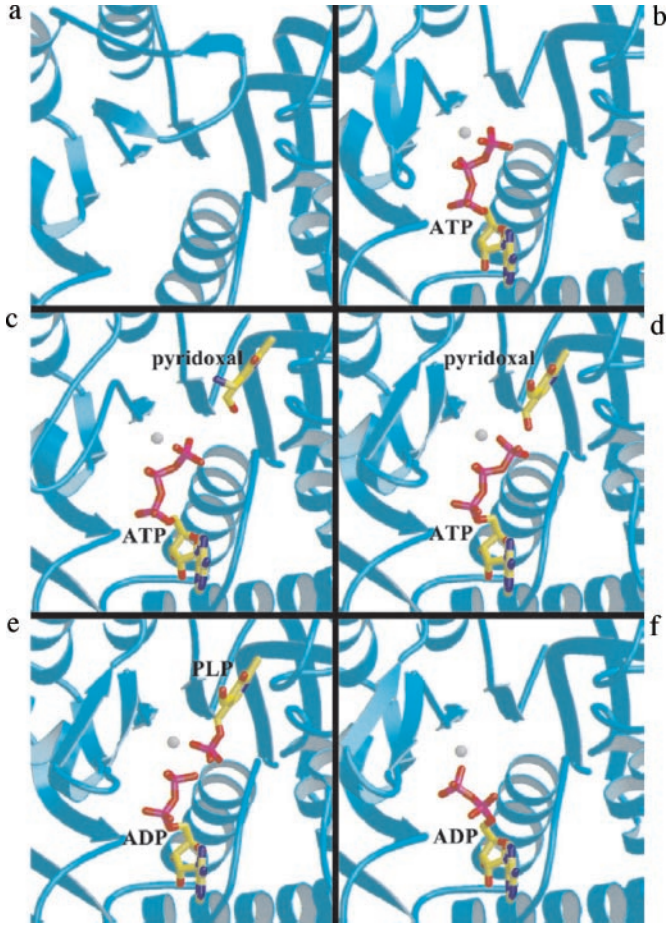

FIG. 6. **The entire process of pyridoxal kinase catalysis.** *a*, the active site of PLK without any substrate bound to it (drawn according to the crystal structure of PLK). *b*, after the binding of ATP, a loop undergoes remarkable conformational changes and interacts with the ATP (drawn according the crystal structure of the PLK·ATP complex). *c*, when ATP and pyridoxal are both bound in the enzyme, they are far away from each other and no significant changes occur on the overall structure of PLK (drawn according to the crystal structure of the PLK·AMP-PCP-pyridoxamine complex with AMP-PCP replaced by ATP and pyridoxamine replaced by pyridoxal). *d*, the active site becomes more compact and binds the substrates more tightly. The two substrates move close to each other, and their reaction groups are located in the catalyzing position (drawn according to the proposed pre-reaction state model). *e*, phosphate transfer occurs, resulting in two substrates, ADP and PLP (drawn according to the crystal structure of the PLK·ADP·PLP complex). *f*, one of the two substrates, PLP, has been released from the enzyme. The active site is open again, and the conformation of ADP is different from the conformation of the PLK·ADP·PLP complex. The ADP leaves the enzyme after which new substrates will be bound (drawn according to the crystal structure of the PLK·ADP complex).

that the hydroxyl oxygen atom can spontaneously attack the γ-phosphate of ATP. This mechanism is carried out primarily by the side chain carboxyl group of Asp-235 in PLK. Another mechanism is carried out by other kinases in the ribokinase superfamily. For example, a positively charged residue, such as Lys-43 in ribokinase or Arg-136 in adenosine kinase, exerts a stabilizing effect on the γ-phosphate of ATP before transfer of the phosphate group. However, this positively charged residue was not found in the active site of PLK. Arg-120, the only possible residue located near the active site did not interact with ATP or ADP phosphate, suggesting that a positively charged amino acid is not present for the positioning or stabilization of the γ-phosphate. In contrast, the correct positioning of the reaction groups of substrates in PLK relies on extensive interactions between amino acid residues of the enzyme and

substrates. During the time when conformational changes occurred in the enzyme-substrate ternary complex, converting the complex from its initial state to the pre-reaction state, amino acid residues of PLK would move toward the active site and cause movement toward the substrates through several interactions described above. As a result, substrates bound to the protein became more rigid than before (Fig. 4*b*). A comparison of the structures of the PLK·AMP-PCP-pyridoxamine complex and pre-reaction state model showed that the number of atom pairs with distances <4 Å between pyridoxal and protein increased from 29 to 46 and the number of atom pairs with short distances increased from 70 to 99. A decrease in the distance between atom pairs leads to a further decrease in the volume of an active site, leaving limited free space around the substrates inside the site. As a result, both substrates in this pre-reaction state could be completely buried (Fig. 4*c*) in the protein mass. By limiting the substrate in a restricted space, this phenomenon directed the reaction group, the γ-phosphate of ATP, and the 5′-hydroxyl group of pyridoxal to collide with each other, allowing the reaction to occur. The positioning and directing of substrates by cooperative conformational changes in the overall protein structure of enzymes is unique in the catalytic mechanism of PLK.

CONCLUSION

The Overall Catalyzing Process of PLK—Crystallographic studies of PLK with respect to the binary and ternary complex of enzyme in the presence of substrates and products provide information for the elucidation of an integral mechanism in the catalytic process carried out by PLK.

Initially, PLK exhibits an open conformation before the binding of any substrate. This exposes the ATP binding site to the solution of the reaction medium but does not expose the pyridoxal binding site (observed in the PLK structure and shown in Fig. 6*a*).

After ATP is bound to the enzyme, the overall structure of PLK changes little at this stage. The loop over the pyridoxal binding site then swings onto the ATP binding site and interacts with the ATP phosphate. At this time, the ATP γ-phosphate is far away from the catalytic site of PLK to prevent hydrolysis (observed in the structure of PLK·ATP complex and shown in Fig. 6*b*). These procedural incidents are consistent with the random substrate binding kinetics followed by PLK.

When pyridoxal as a vitamin B_6 substrate binds to the enzyme, conformational changes of amino acid residues localized at the pyridoxal binding site cause the protein to become more compact than its normal state, enabling the substrate to be tightly bound. Interestingly, this conformational change does not extend to the ATP binding site maintaining the ATP γ-phosphate far away from the catalytic site (observed in the structure of PLK·AMP-PCP-pyridoxamine complex and shown in Fig. 6*c*). The existence of such a stage in the catalytic mechanism of PLK may be related to the regulation of PLK through other proteins. Previous reports have shown that PLK could form complexes with some PLP-binding enzymes such as aspartate aminotransferase and pyridoxine-5-phosphate oxidase (24, 27) to restrict the release of free PLP into the cellular environment where phosphatases are present. It is possible that the binding of these proteins to PLK may accelerate further conformational changes in the enzyme and lead to spontaneous enzymatic reactions. However, investigation of this particular aspect is needed for further understanding of the mechanism behind protein-protein interactions between PLK and other binding proteins.

Later on, further conformational changes cause the structure to become more compact and reach the pre-reaction state and both substrates are pushed by the surrounding amino acid residues to move to positions where their reaction groups are close to each other. This movement causes the ATP γ-phosphate to be stabilized by an anion hole in the active site, and the pyridoxal 5′-hydroxyl group forms a hydrogen bond with the side chain carboxyl group of Asp-235 (Fig. 6*d*). Electrons of the oxygen atom of the 5′-hydroxyl group starts a nucleophilic attack on the phosphorus atom γ-phosphate of ATP, forming a new bond. The phosphorus atom in the γ-position then moves a distance of 0.8 Å, causing the bond between it and the β-phosphate group to break. Thus, the phosphate transfer is completed and the two products, ADP and PLP, are generated (observed in the structure of PLK·ADP·PLP complex and shown in Fig. 6*e*).

To release reaction products, the overall conformation of the enzyme relaxes again. The active site is exposed to the reaction medium solution, which allows the products to be released as free molecules (observed in the structure of the PLK·ADP complex and shown Fig. 6*f*). For the second catalytic cycle to start, PLK can accept new substrates again for the next cycle of catalysis.

REFERENCES

1. Kerry, J. A., Rohde, M., and Kwok, F. (1986) *Eur. J. Biochem.* **158,** 581–585
2. McCormick, D. B., and Snell, E. E. (1959) *Proc. Natl. Acad. Sci. U. S. A.* **45,** 1371–1379
3. McCormick, D. B., and Snell, E. E. (1961) *J. Biol. Chem.* **263,** 2085–2088
4. Hanna, M. C., Turner, A. J., and Kirkness, E. F. (1997) *J. Biol. Chem.* **272,** 10756–10760
5. Yang, Y., Zhao, G., and Winkler, M. E. (1996) *FEMS Microbiol Lett.* **141,** 89–95
6. Yang, Y., Tsui, H. C., Man, T. K., and Winkler, M. E. (1998) *J. Bacteriol.* **180,** 1814–1821
7. Li, M.-H., Kwok, F., Chang, W.-R., Lau, C.-K., Zhang, J.-P., Lo, S. C. L., Jiang, T., and Liang, D.-C. (2002) *J. Biol. Chem.* **277,** 46385–46390
8. Sigrell, J. A., Cameron, A. D., Jones, T. A., and Mowbray, S. L. (1998) *Structure* **6,** 183–193
9. Mathews, I. I., Erion, M. D., and Ealick, S. E. (1998) *Biochemistry* **37,** 15607–15620
10. Schumacher, M. A., Scott, D. M., Mathews, I. I., Ealick, S. E., Roos, D. S., Ullman, B., and Brennan, R. G. (2000) *J. Mol. Biol.* **298,** 875–893
11. Campobasso, N., Mathews, I. I., Begley, T. P., and Ealick, S. E. (2000) *Biochemistry* **39,** 7868–7877
12. Ito, S., Fushinobu, S., Yoshioka, I., Koga, S., Matsuzawa, H., and Wakagi, T. (2001) *Structure* **9,** 205–214
13. Cheng, G., Bennett, E. M., Begley, T. P., and Ealick, S. E. (2002) *Structure* **10,** 225–235
14. Sigrell, J. A., Cameron, A. D., and Mowbray, S. L. (1999) *J. Mol. Biol.* **290,** 1009–1018
15. Li, M.-H., Kwok, F., An, X.-M., Chang, W.-R., Lau, C.-K., Zhang, J.-P., Liu, S.-Q., Leung, Y.-C., Jiang, T., and Liang, D.-C. (2002) *Acta Crystallogr. D* **58,** 1479–1481
16. Otwinowski, Z. (1993) in *Proceedings of the CCP4 Study Weekend* (Issacs, N., Bailey, S., and Sawyer, L.) pp. 56–62, Daresbury Laboratories, Warrington, United Kingdom
17. Navaza, J., and Saludjian, P. (1997) *Methods Enzymol.* **276,** 581–594
18. Yeates, T. O. (1997) *Methods Enzymol.* **276,** 344–358
19. Vagin, A., and Teplyakov, A. (1997) *J. Appl. Crystallogr.* **30,** 1022–1025
20. Brunger, A. T., Adams, P. D., Clore, G. M., DeLano, W. L., Gros, P., Grosse-Kunstleve, R. W., Jiang, J. S., Kuszewski, J., Nilges, M., Pannu, N. S., Read, R. J., Rice, L. M., Simonson, T., and Warren, G. L. (1998) *Acta Crystallogr. D* **54,** 905–921
21. Brunger, A. T., Krukowski, A., and Erickson, J. W. (1991) *Acta Crystallogr. A* **46,** 585–593
22. Jones, T. A., Zuo, J. Y., Cowan, S. W., and Kjeldgaard, M. (1991) *Acta Crystallogr. A* **47,** 110–119
23. Laskowski, R. A., MacArthur, M. W., Moss, D. S., and Thornton, J. M. (1993) *J. Appl. Crystallogr.* **26,** 283–291
24. Kwok, F., and Churchich, J. E. (1980) *J. Biol. Chem.* **255,** 882–887
25. Kraulis, P. J. (1991) *J. Appl. Crystallogr.* **24,** 946–950
26. Merritt, E. A., and Bacon, D. J. (1997) *Methods Enzymol.* **277,** 505–524
27. Kim, Y. T., Kwok, F., and Churchich, J. E. (1988) *J. Biol. Chem.* **263,** 13712–13717